# Ca$^{2+}$-Permeable Channels/Ca$^{2+}$ Signaling in the Regulation of Ileal Na$^{+}$/Gln Co-Transport in Mice

Fenglan Chu[1†], Hanxing Wan[2†], Weidong Xiao[3], Hui Dong[2]* and Muhan Lü[1]*

[1]Department of Gastroenterology, Affiliated Hospital of Southwest Medical University, Luzhou, China, [2]Department of Gastroenterology, Xinqiao Hospital, Army Medical University, Chongqing, China, [3]Department of General Surgery, Xinqiao Hospital, Army Medical University, Chongqing, China

Oral glutamine (Gln) has been widely used in gastrointestinal (GI) clinical practice, but it is unclear if Ca$^{2+}$ regulates intestinal Gln transport, although both of them are essential nutrients for mammals. Chambers were used to determine Gln (25 mM)-induced $I_{sc}$ through Na$^{+}$/Gln co-transporters in the small intestine in the absence or the presence of selective activators or blockers of ion channels and transporters. Luminal but not serosal application of Gln induced marked intestinal $I_{sc}$, especially in the distal ileum. Lowering luminal Na$^{+}$ almost abolished the Gln-induced ileal $I_{sc}$, in which the calcium-sensitive receptor (CaSR) activation were not involved. Ca$^{2+}$ removal from both luminal and serosal sides of the ileum significantly reduced Gln- $I_{sc}$. Blocking either luminal Ca$^{2+}$ entry via the voltage-gated calcium channels (VGCC) or endoplasmic reticulum (ER) release via inositol 1,4,5-triphosphate receptor (IP$_{3}$R) and ryanodine receptor (RyR) attenuated the Gln-induced ileal $I_{sc}$, Likewise, blocking serosal Ca$^{2+}$ entry via the store-operated Ca$^{2+}$ entry (SOCE), TRPV1/2 channels, and Na$^{+}$/Ca$^{2+}$ exchangers (NCX) attenuated the Gln-induced ileal $I_{sc}$. In contrast, activating TRPV1/2 channels enhanced the Gln-induced ileal $I_{sc}$. We concluded that Ca$^{2+}$ signaling is critical for intestinal Gln transport, and multiple plasma membrane Ca$^{2+}$-permeable channels and transporters play roles in this process. The Ca$^{2+}$ regulation of ileal Na$^{+}$/Gln transport expands our understanding of intestinal nutrient uptake and may be significant in GI health and disease.

Keywords: calcium signaling, VGCC, SOCE, CICR, TRPV, NCX

## INTRODUCTION

Glutamine (Gln) is the most abundant free amino acid (AA) in mammalian plasma and is traditionally considered a non—essential amino acid. Gln is also the most widely used AA in clinical practice, such as in weaning, pregnancy, various gastrointestinal (GI) diseases, as well as the intestinal injury caused by burning (Shi et al., 2018), infection (Liu et al., 2017), and tumor treatment (Takechi et al., 2014) when endogenous Gln is in short supply under some physiological or pathological conditions. Moreover, Gln is regarded as an essential nutritional AA for newborns and a conditional essential AA for adults (Wang et al., 2015). During periods of increased intestinal stress, Gln can stimulate intestinal nutrient absorption while maintaining mucosal barrier function and promoting mucosal growth (Chen et al., 2018; Li et al., 2019). Therefore, investigation on the regulation of Gln uptake will further promote our understanding of its role in GI health and therapeutic application in GI diseases.

**FIGURE 1 |** Luminal Gln is transported mainly in the ileum through NGcT. **(A)** Representative time courses of mucosal addition (indicated by the blue arrow) of Gln (25 mM)-stimulated $I_{sc}$ of the duodenum, proximal jejunum, and distal ileum. **(B)** Comparisons of Gln-stimulated $I_{sc}$ rising rates when added to the mucosal (m) side among different segments of the intestine ($n = 6$). **(C)** Representative examples of dose-response relations for adding Gln (1–50 mM) to the ileum mucosal side. ($n \geq 6$). **(D)** Representative time courses of Gln (25 mM)-stimulated $I_{sc}$ and the summary data of $I_{sc}$ peak when added (indicated by the blue arrow) to the serosal (s) or mucosal (m) side of the ileum ($n = 6$). **(E)** Comparison of the distal ileum $I_{sc}$ induced by mucosal side addition of Gln (25 mM) in mucosal normal Na⁺ condition (Ctrl, $n \geq 6$) or the low-Na⁺ condition [low Na⁺ (m), Li⁺ replaced Na⁺, n = 6]. **(F)** Representative time courses and summary data of Gln (5 mM)- stimulated $I_{sc}$ peak in the absence (Ctrl, $n \geq 6$) or the presence of cinromide (Cin(m), 25 μM, $n = 6$) added (indicated by the red arrow) to mucosal side of the ileum. **(G)** Representative time courses and summary data of Gln (5 mM) stimulated the $I_{sc}$ peak in the absence (Ctrl, $n \geq 6$) or the presence of GPNA (200 μM, $n = 6$) added (indicated by the red arrow) to mucosal side of the ileum. Results are presented as mean ± S.E. NS, no significant differences, **$p < 0.01$, ***$p < 0.001$, ****$p < 0.0001$ vs. corresponding control by one-way ANOVA followed Dunnett's post-test.

Gln transporters can be divided into Na⁺-dependent transporters and Na⁺-independent transporters. Na⁺-dependent transporters expressed differently in different organs, tissues, and cells (Oguchi et al., 2012; Leke et al., 2015; Yamada et al., 2019). Gln is mainly absorbed by Na⁺/Gln co-transporters (NGcT) in the proximal jejunum and ileum. So far, the intestinal NGcT have been classified as follows: system A (SNAT1/2/4), system ASC(ASCT2), system B⁰(B⁰AT1), system B⁰,⁺ (ATB⁰,⁺), system N(SNAT3/5/7), and system y⁺L (y⁺LAT1/2). ATB⁰,⁺and ASCT2 were lowly expressed in the small intestines but high in the large intestines, while the rest were mainly expressed in the small intestine. System A and y⁺L are mainly localized basolaterally in the intestinal epithelium, whereas most of the others are at the apical (Broer and Fairweather 2019). The Na⁺-independent Gln transporters include system asc (Asc-1), b⁰,⁺ (b⁰,⁺AT), and L (LAT1/2), in which Gln is

transported by exchange with other AA or ions. Although Gln transport pathways, kinetic properties, and energy requirements in different cells and animal models have been extensively investigated, few studies have described the short-term regulation of Gln transport across intestinal epithelial cells (IEC).

As an important second messenger, Ca²⁺ is involved in various physiological processes, such as muscle contraction, hormone secretion, and neurotransmitter release. We have previously reported Ca²⁺ signaling regulation of ion secretion and absorption through SGLT1 in the intestinal epithelium (Zhang F. et al., 2019; Yinghui et al., 2021, Zhang et al., 2021). We also revealed that Ca²⁺ signaling regulates H⁺/peptide transporter PEPT1 to mediate intestinal Gly-Sar uptake in mice (Xu et al., 2020). However, it is currently unknown if Ca²⁺ signaling regulates intestinal Gln uptake.
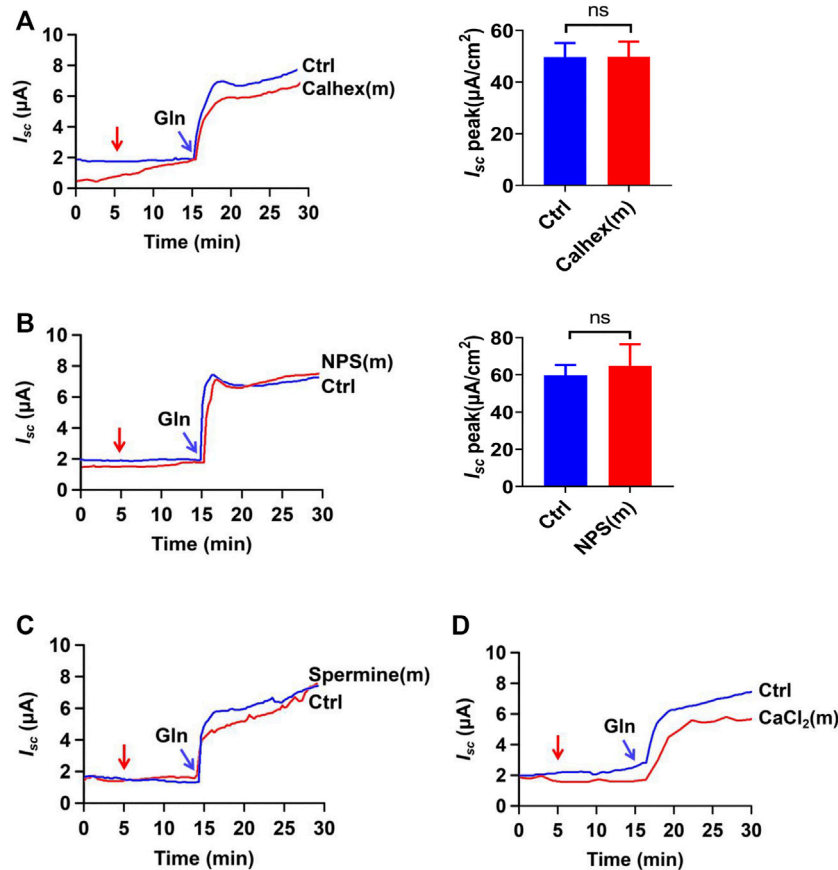
**FIGURE 2** | Gln-induced ileal $I_{sc}$ is not mediated by CaSR activation. **(A)** Representative time courses and summary data showing the effect of mucosal (m) addition of Calhex 231 (Calhex, 10 μM, n = 5) on Gln (5 mM)-stimulated $I_{sc}$. The red arrow indicates the time of drug addition. Ctrl (n ≥ 6) represents the control without drug treatment. **(B)** Representative time courses and summary data of Gln (25 mM)-stimulated $I_{sc}$ after mucosal addition of NPS-2143 (NPS, 30 μM, n = 5). The red arrow indicates the time of drug addition. Ctrl (n ≥ 6) is the control group without drug treatment. **(C)** Representative time courses showing the effect of mucosal addition of spermine (3 mM) (indicated by the red arrow) on Gln (5 mM)-stimulated $I_{sc}$. **(D)** Representative time courses showing the effect of mucosal addition of CaCl₂ (5 mM) (indicated by the red arrow) on Gln-stimulated $I_{sc}$. Results are presented as mean ± S.E. NS, no significant differences vs. corresponding control by Student's unpaired, two-tailed $t$-test.

Given that $Ca^{2+}$ appears to regulate diverse intestinal nutrient uptake, it is reasonable to speculate that $Ca^{2+}$ may also regulate Gln transporters in the gut. Moreover, Gln can enhance intestinal $Ca^{2+}$ absorption, and intracellular $Ca^{2+}$ is involved in the intestinal cell protective effect of Gln (Okuda et al., 2006; Moine et al., 2017), indicating an interaction of intracellular $Ca^{2+}$ and Gln. Therefore, Gln and $Ca^{2+}$ in the intestinal epithelia might be mutually reinforcing feedback loops, although the specific mechanisms and molecular components involved are still unclear. Taking into account the above, the purpose of this study is to determine whether $Ca^{2+}$ signaling can regulate the transport of intestinal Gln in experimental animals and the underlying molecular mechanisms.

# MATERIALS AND METHODS

## Animals

Harlan C-57BL/6 male mice were aged 6–8 weeks, weighing 21–23 g (purchased from Chongqing Tengxin Biotechnology Co., Ltd., Chongqing, China) were selected for the experiment. Mice were fed in a standard animal feeding room with an ambient temperature of 20–30°C, a humidity of 50–55%, a light/dark cycle for 12 h, and a free choice of food/water. All animal experiments complied with the requirements of the University's Animal Ethics Committee and were approved by the University's Animal Research Committee. The animals were randomly selected and aggregated in all experiments, and the data were collected and assessed blindly. The animals were killed when they sprained their necks under $CO_2$ anesthesia.

## Tissue Preparation

After killing the animals as described above, the abdomen was opened layer by layer along the midabdominal line. In this study, the duodenum, proximal jejunum, or distal ileum mucosal tissues were mainly intercepted, with a length of about 5 cm. To ensure intestinal epithelial activity and avoid further damage, isolated intestinal segments were incubated in a 10 ml cold isotonic mannitol (300 mM)
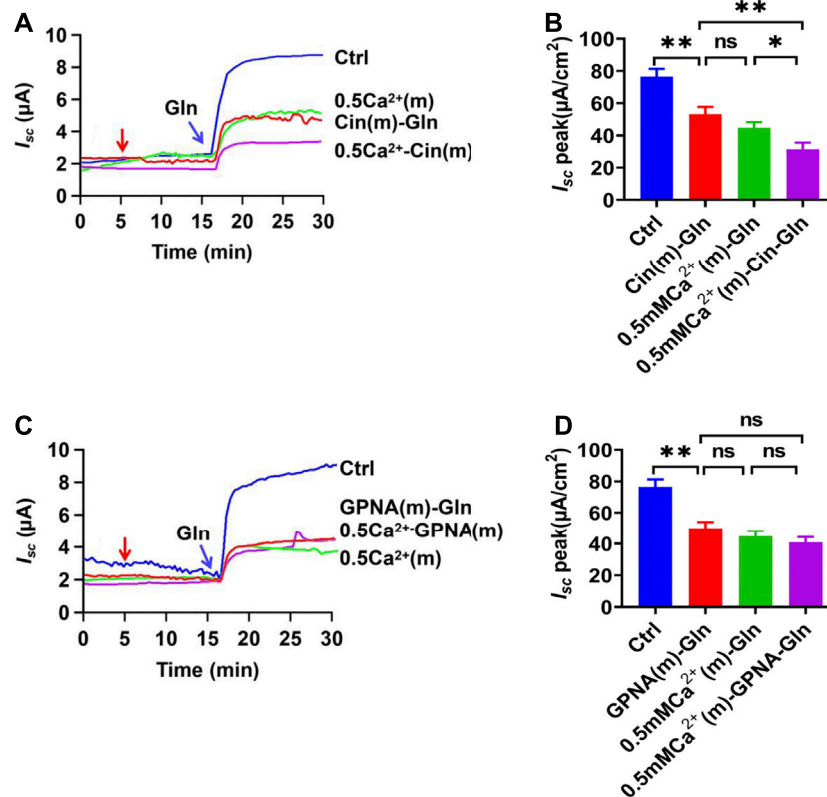
**FIGURE 3 |** Gln ileal transport is luminal $Ca^{2+}$-dependent. **(A)** Representative time courses showing the effect of reduced $Ca^{2+}$ concentration in mucosal side [0.5 mM $Ca^{2+}$ (m)-Gln] and the addition of cinromide (add at the red arrow) on Gln (5 mM)-stimulated $I_{sc}$. Ctrl represents Gln-induced $I_{sc}$ at the normal $Ca^{2+}$ concentration (1.2 mM $Ca^{2+}$) on the mucosal side without any treatment. **(B)** Summary data of Gln-stimulated $I_{sc}$ after mucosal addition of single 25 μM Cinromide [Cin (m)-Gln, $n = 7$], single reduced mucosal $Ca^{2+}$ [0.5 $Ca^{2+}$ (m)-Gln, $n = 6$], or both of them [0.5 mM $Ca^{2+}$ (m) -Cin-Gln, $n = 6$]. Compared with Gln (Ctrl, 5 mM, $n \geq 6$) induced $I_{sc}$ without any treatment. **(C)** Representative time courses of Gln (5 mM) -stimulated $I_{sc}$ after $Ca^{2+}$ reduction [0.5 $Ca^{2+}$(m)], and addition of GPNA (add at the red arrow) to normal $Ca^{2+}$ or 0.5 mM $Ca^{2+}$ solutions. Ctrl represents the control without any treatment. **(D)** Summary data of Gln-stimulated $I_{sc}$ after mucosal addition of single GPNA [GPNA (m)-Gln, $n = 6$], single reduced mucosal $Ca^{2+}$ [0.5 mM $Ca^{2+}$ (m), $n = 6$], or the presence of GPNA (500 μM) in lower $Ca^{2+}$ condition [0.5 mM $Ca^{2+}$ (m)-GPNA-Gln, $n = 6$]. Compared with Gln-induced $I_{sc}$ without any treatment. Results are presented as mean ± S.E. NS, no significant differences, *$p < 0.05$, **$p < 0.01$, ***$p < 0.001$ *vs*. corresponding control by Student's unpaired, one-way ANOVA followed Dunnett's post-test.

solution containing 10 μM indomethacin for 10 min. The intestinal tract was then opened longitudinally along with the mesentery. Food scraps were removed by scrubbing in the buffer, then dissected to remove the overlying smooth muscle and associated intermuscular nerves. Finally, segments were divided it into 3–4 chamber-sized tissues (window area, 0.1 cm²).
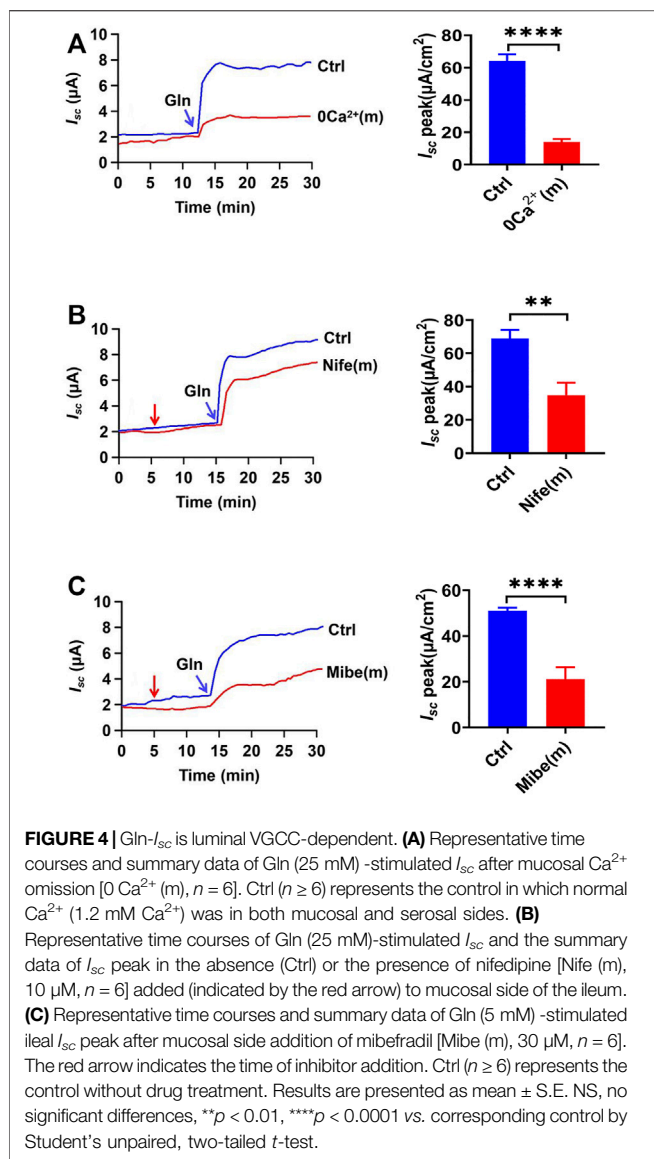
## Ussing Chamber Experiments

The treated mucosa of the small intestine was attached between chambers with an exposed area of 0.1 cm². Experiments were performed under continuous short-circuited conditions (Voltage-Current Clamp, VCC MC6; Physiologic Instruments, San Diego, CA). After 15–30 min of basic parameters measurement, Gln was added to the mucosal side chamber of the tissue. When screening for molecular components, different drugs were added to the mucosal, serosal, or bilateral side for 10–20 min, followed by adding Gln. The transepithelial short-circuit currents ($I_{sc}$) were measured *via* an automatic voltage

clamp, in which μA was used for the original recordings, but μA/cm² was used for summary data.

## Solution

The buffer solution on both sides of the Ussing chamber was prepared separately. The components of the mucosal solution (mM) were 115 NaCl, 1.2 $MgCl_2$, 1.2 $CaCl_2$, 25 sodium gluconate, 5.2 potassium gluconate, and 10 D-mannitol (final PH of 7.4) and gassed with 100% oxygen. Composition of serosal solution (mM): 115 NaCl, 1.2 $MgCl_2$, 1.2 $CaCl_2$, 25 $NaHCO_3$, 2.2 $K_2HPO_4$, 0.8 $KH_2PO_4$, and 10 D-glucose (final PH of 7.4) in a carbon-oxygen mixture (5% $CO_2$ and 95% $O_2$, v/v). In the experiment, 3 ml of the above-mentioned solution were added to either side of the chamber at a constant temperature of 37°C. To create a low $Na^+$ environment on the mucosal side, the $Na^+$ in the mucosal solution was replaced with $Li^+$ at the same concentration. For the low $Ca^{2+}$ experiment, the concentration of $CaCl_2$ was reduced to 0.5 mM; In the zero-$Ca^{2+}$ experiment, $Ca^{2+}$ in the solution was omitted, and EGTA (0.5 mM) was

**FIGURE 4** | Gln-$I_{sc}$ is luminal VGCC-dependent. **(A)** Representative time courses and summary data of Gln (25 mM) -stimulated $I_{sc}$ after mucosal Ca²⁺ omission [0 Ca²⁺ (m), $n$ = 6]. Ctrl ($n$ ≥ 6) represents the control in which normal Ca²⁺ (1.2 mM Ca²⁺) was in both mucosal and serosal sides. **(B)** Representative time courses of Gln (25 mM)-stimulated $I_{sc}$ and the summary data of $I_{sc}$ peak in the absence (Ctrl) or the presence of nifedipine [Nife (m), 10 µM, $n$ = 6] added (indicated by the red arrow) to mucosal side of the ileum. **(C)** Representative time courses and summary data of Gln (5 mM) -stimulated ileal $I_{sc}$ peak after mucosal side addition of mibefradil [Mibe (m), 30 µM, $n$ = 6]. The red arrow indicates the time of inhibitor addition. Ctrl ($n$ ≥ 6) represents the control without drug treatment. Results are presented as mean ± S.E. NS, no significant differences, **$p$ < 0.01, ****$p$ < 0.0001 $vs.$ corresponding control by Student's unpaired, two-tailed $t$-test.

added to prevent potential Ca²⁺ contamination. Such solutions were isotonic for tissues.

## Materials

Sigma (Saint Louis, MO, United States) supplied L-Glutamine, spermine, cyclopiazonic acid (CPA), nifedipine, and gadolinium (III) chloride (GdCl₃). GPNA hydrochloride, cinromide, Calhex 231 hydrochloride, NPS-2143, AMG 517, N, N, N′, N′- tetrakis (2-pyridylmethyl) ethylenediamine (TPEN), probenecid, SN-6, ouabain, mibefradil, and GSK-7975A were purchased from MedChemExpress (MCE; Monmouth Junction, NJ). Tocris Bioscience (Ellisville, MO) supplied 2-Aminoethyl diphenylborinate (2-APB), while APExBIO Technology LLC (Houston, TX) provided dantrolene. The other chemicals were obtained from BBI Life Science (Shanghai, China). Gln, Lithium chloride (LiCl), and Gadolinium (III) chloride (GdCl₃) were dissolved in ultrapure water. Most of the remainder were

prepared with dimethyl sulfoxide (DMSO), and the volume ratio was less than 1:1,000, which did not affect the basic current.

## Data and Statistical Analysis

The data and statistical analysis yield to the recommendations of Frontiers in Pharmacology. All the results were given as means ± SEM of the number of experimental tissues (n). The dose-response relationship of this study was obtained by nonlinear fitting analysis of Logistic curve parameters of experimental data. The net $I_{sc}$ peak is the maximum peak stimulated by the drug minus the base level. Unpaired two-tailed $t$-test or one-way ANOVA was used, followed by Dunnett's post-test to determine the statistical significance of the mean difference between the experimental groups. A follow-up analysis was performed when F reached $p$ < 0.05 (GraphPad Prism 8.0), and there was no significant variance in inhomogeneity. Only a probability $p$ < 0.05 is considered statistically significant.
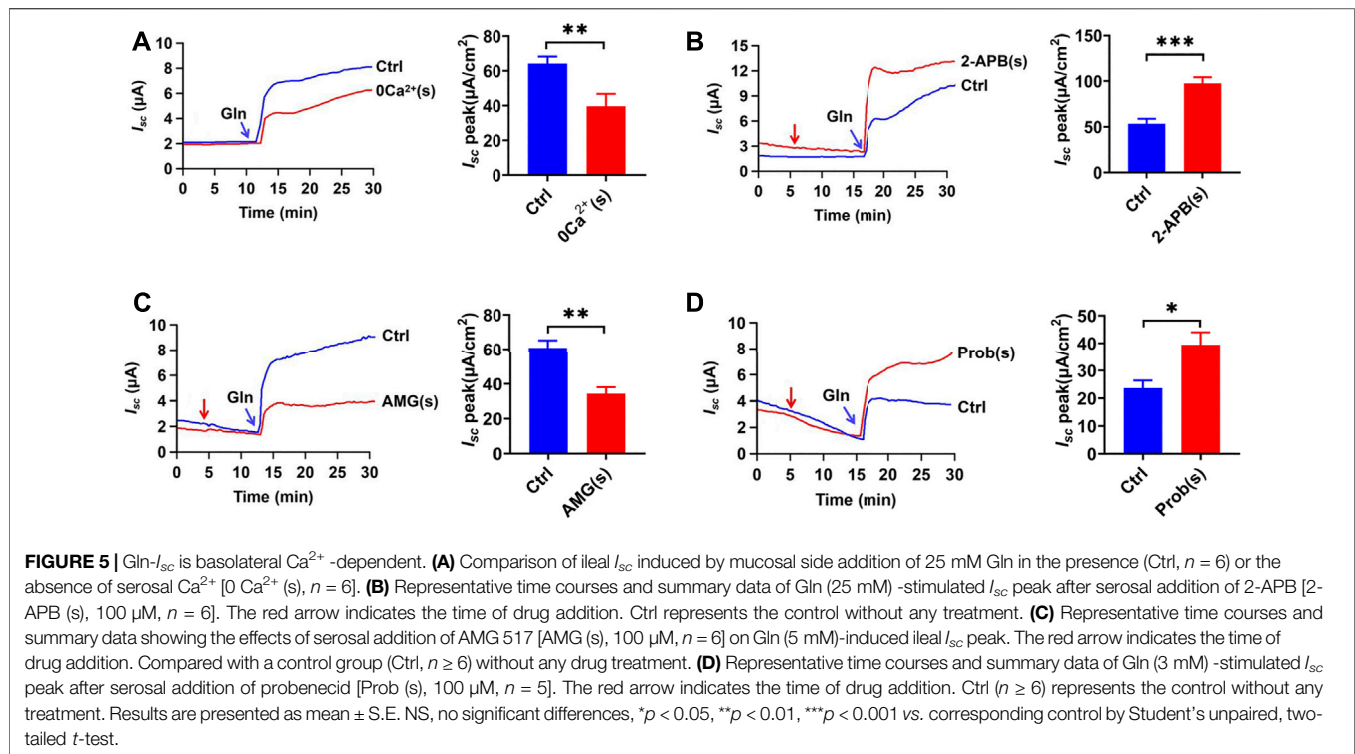
## RESULT

### Gln is Mainly Transported in the Distal Ileum

We used the Ussing chamber experiment to determine if the entry of oral-Gln into the intestinal epithelium is an electrogenic process accompanied by ion transport. Firstly, we found the addition of Gln (25 mM) into the intestinal lumen induced short-circuit current ($I_{sc}$), an instantaneous peak was followed by a continuous-time phase. Secondly, segmental differences in Gln-evoked $I_{sc}$ in the mouse intestine were observed. As shown in **Figure 1A**, Gln induced much greater and faster $I_{sc}$ in the distal ileum than in the proximal jejunum and the duodenum. As depicted in **Figure 1B**, Gln - $I_{sc}$ increased from the proximal to the distal small intestine and mainly transported in the distal ileum. Finally, we analyzed the dose-response curve of ileal Gln-induced $I_{sc}$. A maximum current ($I_{sc}$ max) was 77.59 ± 4.25 µA/cm² and an EC50 was 3 x 10⁻³ M (**Figure 1C**).

### Gln Induces Ileal $I_{sc}$ via the NGcT From the Luminal Side

There are different Gln transporters on IEC's apical and basolateral sides, so we tested which side was involved in Gln transport in the distal ileum. The mucosal application of Gln induced a significant $I_{sc}$, but the serosal application could not induce any detectable $I_{sc}$ (**Figure 1D**), clearly indicating luminal Gln transport. Then reducing the concentration of Na⁺ in mucosal solution significantly reduced the Gln-induced $I_{sc}$ compared to the control group, indicating that intestinal Gln transport requires Na⁺ to be accompanied, namely the luminal Na⁺/Gln co-transporters (NGcT) (**Figure 1E**). Finally, either cinromide (25 µM), a selective inhibitor of epithelial NGcT (B⁰AT1) (Danthi et al., 2019), or GPNA (200 µM), a non-specific inhibitor of NGcT (Broer et al., 2016), attenuated Gln (5 mM)-stimulated $I_{sc}$ peak after it was added to the mucosal side (**Figures 1F,G**).

**FIGURE 5 |** Gln-$I_{sc}$ is basolateral Ca²⁺-dependent. **(A)** Comparison of ileal $I_{sc}$ induced by mucosal side addition of 25 mM Gln in the presence (Ctrl, $n = 6$) or the absence of serosal Ca²⁺ [0 Ca²⁺ (s), $n = 6$]. **(B)** Representative time courses and summary data of Gln (25 mM) -stimulated $I_{sc}$ peak after serosal addition of 2-APB [2-APB (s), 100 µM, $n = 6$]. The red arrow indicates the time of drug addition. Ctrl represents the control without any treatment. **(C)** Representative time courses and summary data showing the effects of serosal addition of AMG 517 [AMG (s), 100 µM, $n = 6$] on Gln (5 mM)-induced ileal $I_{sc}$ peak. The red arrow indicates the time of drug addition. Compared with a control group (Ctrl, $n \geq 6$) without any drug treatment. **(D)** Representative time courses and summary data of Gln (3 mM) -stimulated $I_{sc}$ peak after serosal addition of probenecid [Prob (s), 100 µM, $n = 5$]. The red arrow indicates the time of drug addition. Ctrl ($n \geq 6$) represents the control without any treatment. Results are presented as mean ± S.E. NS, no significant differences, *$p < 0.05$, **$p < 0.01$, ***$p < 0.001$ vs. corresponding control by Student's unpaired, two-tailed $t$-test.

## The CaSR Activation is not Involved in the Ileal Na⁺/Gln Co-Transport

In addition to the Na⁺-coupled Gln transporters, the calcium-sensitive receptors (CaSR) may be activated by Gln as an L-amino acid to participate in intestinal Gln response via Gq/Ca²⁺ signaling pathway (Joshi et al., 2013). To examine whether the CaSR activation is involved in ileal Gln-induced $I_{sc}$, calhex 231 (10 µM) and NPS-2143 (30 µM), two selective CaSR antagonists, were first applied; but neither of them altered the ileal Gln-induced $I_{sc}$ (**Figures 2A,B**). Secondly, spermine (3 mM) and CaCl₂ (5 mM), two CaSR activators, did not induce any currents by themselves; nor did they affect the Gln-induced ileal $I_{sc}$ (**Figures 2C,D**). These data clearly exclude the involvement of the CaSR in the Gln-induced ileal $I_{sc}$ or Na⁺/Gln co-transport.

## Luminal Ca²⁺ is Required for Ileal NGcT

To investigate whether luminal Ca²⁺ is important in Na⁺/Gln co-transport, extracellular Ca²⁺ on the mucosal side was reduced to a low Ca²⁺ concentration (0.5 mM). As shown in **Figures 3A,B**, Gln-induced $I_{sc}$ was significantly reduced in low Ca²⁺ concentration, suggesting its important role. Interestingly, luminal addition of cinromide further reduced Gln-induced $I_{sc}$ in low Ca²⁺ concentration (**Figures 3A,B**), but GPNA did not (**Figures 3C,D**), suggesting that the sensitivities of NGcT to luminal Ca²⁺ may be different.

To further study the role of Ca²⁺ in Na⁺/Gln co-transport, luminal Ca²⁺ was omitted. Ca²⁺ omission almost abolished Gln-induced $I_{sc}$ (**Figure 4A**), indicating that luminal Ca²⁺ is not only

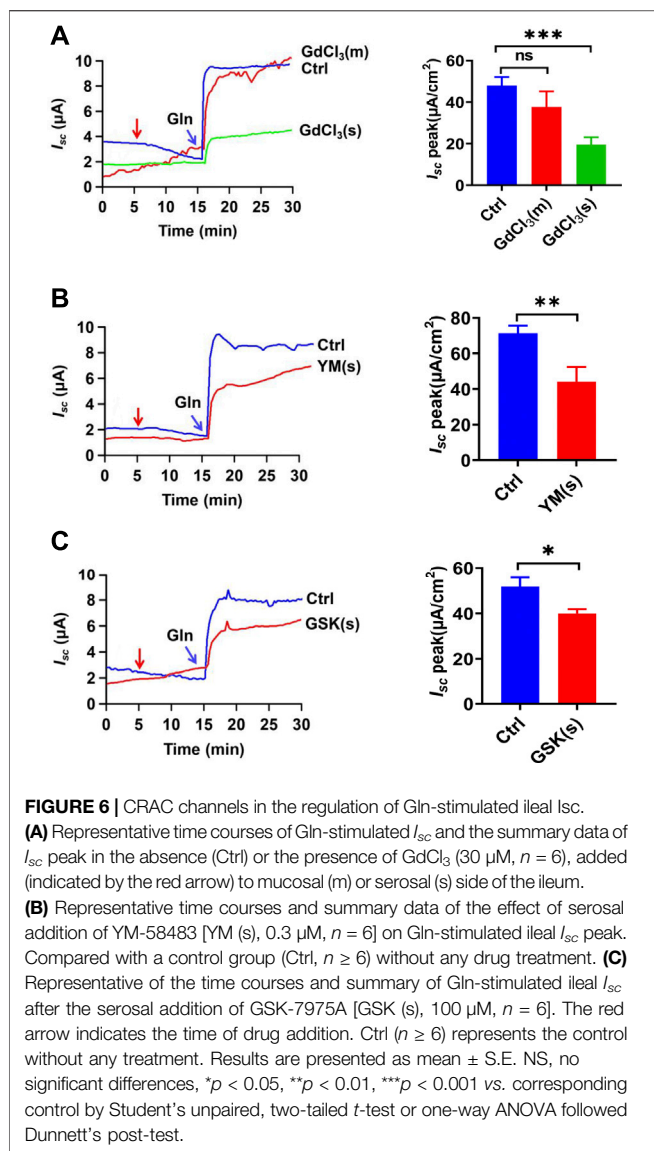vital in ileal Gln electrogenic transport but also dose-dependently regulates this process.

## Role of Luminal Ca²⁺ Entry via the VGCC in Ileal Na⁺/Gln Co-Transport

To elucidate the mechanisms of how luminal Ca²⁺ regulates ileal Gln electrogenic transport, we analyzed the role of Ca²⁺ channels in the regulation of Gln-induced $I_{sc}$. Luminal addition of nifedipine (10 µM), a selective blocker of the L-type voltage-gated Ca²⁺ channels (VGCC), significantly inhibited Gln-induced $I_{sc}$ (**Figure 4B**). In addition, mibefradil (30 µM), a selective blocker of the T-type VGCC (Mehrke et al., 1994), also inhibited Gln-induced ileal $I_{sc}$ after added to the luminal side (**Figure 4C**). Therefore, luminal Ca²⁺ influx via VGCC is critical for ileal Na⁺/Gln co-transport.

## Role of Serosal Ca²⁺ Entry via TRPV Channels in Gln-$I_{sc}$

To examine whether serosal Ca²⁺ also participates in Gln ileal response, we investigated the Gln-evoked $I_{sc}$ after omitting serosal Ca²⁺. As shown in **Figure 5A**, serosal Ca²⁺ omission markedly inhibited Gln-evoked $I_{sc}$, indicating the importance of serosal Ca²⁺.

Since TRPV as Ca²⁺-permeable channels are expressed and function in the ileum (Allais et al., 2020; Manneck et al., 2021), we tested whether Ca²⁺ influx via the TRPV channels on the serosal side regulates Na⁺/Gln co-transport. Firstly, serosal application of 2-Aminoethyl diphenylborinate (2-APB) (100 µM) (Hu et al.,

**FIGURE 6 |** CRAC channels in the regulation of Gln-stimulated ileal Isc.
**(A)** Representative time courses of Gln-stimulated $I_{sc}$ and the summary data of $I_{sc}$ peak in the absence (Ctrl) or the presence of GdCl$_3$ (30 μM, $n = 6$), added (indicated by the red arrow) to mucosal (m) or serosal (s) side of the ileum.
**(B)** Representative time courses and summary data of the effect of serosal addition of YM-58483 [YM (s), 0.3 μM, $n = 6$] on Gln-stimulated ileal $I_{sc}$ peak. Compared with a control group (Ctrl, $n \geq 6$) without any drug treatment. **(C)** Representative of the time courses and summary of Gln-stimulated ileal $I_{sc}$ after the serosal addition of GSK-7975A [GSK (s), 100 μM, $n = 6$]. The red arrow indicates the time of drug addition. Ctrl ($n \geq 6$) represents the control without any treatment. Results are presented as mean ± S.E. NS, no significant differences, $*p < 0.05$, $**p < 0.01$, $***p < 0.001$ vs. corresponding control by Student's unpaired, two-tailed $t$-test or one-way ANOVA followed Dunnett's post-test.

2004), an activator of TRPV1/2/3 channels, significantly enhanced Gln-induced ileal $I_{sc}$ (**Figure 5B**). Secondly, serosal application of AMG 517 (100 μM), a selective blocker of TRPV1 channels, significantly attenuated ileal Gln-$I_{sc}$ (**Figure 5C**). Finally, probenecid (100 μM), a selective activator of TRPV2 channels, enhanced Gln-induced $I_{sc}$ (**Figure 5D**). Therefore, serosal Ca²⁺ entry *via* TRPV1/2 channels plays a role in ileal Gln-$I_{sc}$.

## The Serosal SOCE Mechanism in Ca²⁺-Mediated Gln-$I_{sc}$

Since the store-operated Ca²⁺ entry (SOCE) is a well-established mechanism to regulate the Ca²⁺-dependent functions in IEC, including jejunal glucose absorption (Zhang et al., 2021),we examined whether the SOCE mechanism regulates ileal Gln-$I_{sc}$ and started with GdCl$_3$, a commonly used SOCE blocker (Zhu

et al., 2020). As shown in **Figure 6A**, serosal addition but not mucosal addition of GdCl$_3$ (30 μM) inhibited Gln-induced $I_{sc}$, consistently with the previous finding of the serosal localization of the SOCE (Zhang et al., 2021). Secondly, serosal application of YM-58483 (0.3 μM) and GSK-7975A (100 μM), two selective SOCE blockers with different structures, also reduced Gln-$I_{sc}$ (**Figures 6B,C**). Thus, the serosal SOCE mechanism is involved in the Ca²⁺-dependent ileal Gln-$I_{sc}$.

## Role of the ER Ca²⁺ Store in Ileal Na⁺/Gln Co-Transport

We further explored the role of intracellular ER Ca²⁺ in Gln-$I_{sc}$. Firstly, cyclopiazonic acid (CPA), an inhibitor of endoplasmic reticulum calcium ATPase (ERCA), can indirectly deplete the ER Ca²⁺. Either mucosal or serosal application of CPA (30 μM) significantly reduced Gln-stimulated $I_{sc}$ (**Figure 7A**). Secondly, we used N, N, N′, N′-tetrakis (2-pyridylmethyl) ethylenediamine (TPEN), a membrane-permeable ER calcium chelator. TPEN (1 mM) inhibited Gln-$I_{sc}$ (**Figure 7B**). Therefore, The ER Ca²⁺ is required for ileal Na⁺/Gln co-transport.
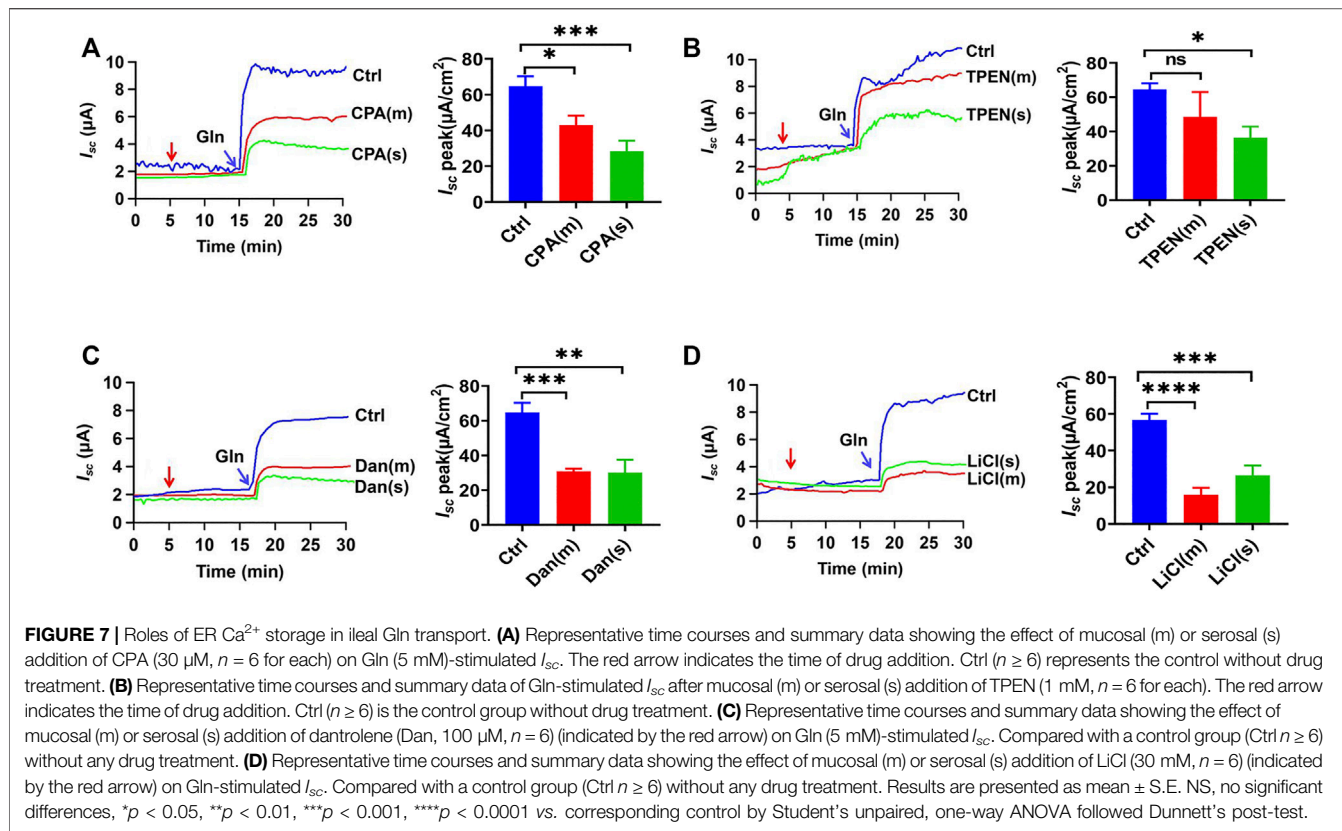
Thirdly, to further explore whether the ER Ca²⁺ release through IP$_3$R and RyR participate in Gln-$I_{sc}$, we applied the selective RyR inhibitor dantrolene (300 μM), which significantly inhibited Gln-induced $I_{sc}$ on each side of the ileum (**Figure 7C**). Moreover, LiCl (30 mM) was used to inhibit IP$_3$ production, and its addition to each side also obviously attenuated Gln-induced $I_{sc}$ (**Figure 7D**). Taken together, the ER Ca²⁺ release *via* IP$_3$R and RyR is required for ileal Na⁺/Gln co-transport.

## The Role of Serosal NKA and NCX in Ileal Gln-$I_{sc}$

Since Na⁺-coupled solute transport across the epithelium requires serosal Na⁺/K⁺ ATPase (NKA) to maintain the transmembrane potential of Na⁺, we tested whether it is involved in ileal Gln-$I_{sc}$. Serosal addition of ouabain (1 mM), a selective inhibitor of NKA, significantly attenuated Gln-induced $I_{sc}$ (**Figure 8A**). We also tested the involvement of the serosal Na⁺/Ca²⁺ exchanger (NCX), a bidirectional transporter of Na⁺ and Ca²⁺. The serosal addition of SN-6 (10 μM), a selective NCX inhibitor, significantly reduced Gln-induced $I_{sc}$ (**Figure 8B**). Therefore, serosal NKA and NCX are involved in ileal Gln-$I_{sc}$.

## DISCUSSION

As Ussing Chamber is widely used to study ion, drug, and nutrient transport in intestinal epithelium (He et al., 2013; Hempstock et al., 2021; Michiba et al., 2021), and we applied it to investigate the regulation of Gln transport. In our study the Gln-induced ileal $I_{sc}$ well represents the Na⁺/Gln co-transport since, 1) the mucosal application of Gln induced a significant $I_{sc}$, but the serosal application could not induce any detectable $I_{sc}$; 2) lowering the concentration of Na⁺ in mucosal solution significantly reduced the Gln-induced $I_{sc}$; 3) either cinromide, a selective inhibitor of epithelial NGcT (B⁰AT1), or GPNA, a

**FIGURE 7** | Roles of ER Ca$^{2+}$ storage in ileal Gln transport. **(A)** Representative time courses and summary data showing the effect of mucosal (m) or serosal (s) addition of CPA (30 μM, $n = 6$ for each) on Gln (5 mM)-stimulated $I_{sc}$. The red arrow indicates the time of drug addition. Ctrl ($n \geq 6$) represents the control without drug treatment. **(B)** Representative time courses and summary data of Gln-stimulated $I_{sc}$ after mucosal (m) or serosal (s) addition of TPEN (1 mM, $n = 6$ for each). The red arrow indicates the time of drug addition. Ctrl ($n \geq 6$) is the control group without drug treatment. **(C)** Representative time courses and summary data showing the effect of mucosal (m) or serosal (s) addition of dantrolene (Dan, 100 μM, $n = 6$) (indicated by the red arrow) on Gln (5 mM)-stimulated $I_{sc}$. Compared with a control group (Ctrl $n \geq 6$) without any drug treatment. **(D)** Representative time courses and summary data showing the effect of mucosal (m) or serosal (s) addition of LiCl (30 mM, $n = 6$) (indicated by the red arrow) on Gln-stimulated $I_{sc}$. Compared with a control group (Ctrl $n \geq 6$) without any drug treatment. Results are presented as mean ± S.E. NS, no significant differences, *$p < 0.05$, **$p < 0.01$, ***$p < 0.001$, ****$p < 0.0001$ vs. corresponding control by Student's unpaired, one-way ANOVA followed Dunnett's post-test.

non-specific inhibitor of NGcT, attenuated Gln-stimulated $I_{sc}$ peak after added to the mucosal side. This notion has been well proved by several previous reports (Rexhepaj et al., 2006; Rexhepaj et al., 2007; Ducroc et al., 2010). Unlike glucose transports, Gln has a diverse and non-selective transport systems. According to expression, distribution and functional specificity of intestinal Gln transporters, our data suggest that NGcT (B$^0$AT1) may play a major role in this process, but the other transporters cannot be ruled out completely (Broer and Fairweather 2019; Chen et al., 2020).

Gln has been widely applied for a long time in clinical practice due to its multiple biological actions in humans. Since most of the Gln in the enteral diet is oxidized and metabolized in the GI tract to produce ATP, it is so-called "intestinal fuel" (Curi et al., 2005). Gln is also an important nitrogen source for synthesizing nucleic acids and proteins that inhibit cell apoptosis and enhance intestinal cell proliferation. Moreover, Gln affects tight junction protein expression and intestinal barrier integrity through Ca$^{2+}$/CaMKK2-AMPK signaling (Wang et al., 2016). In addition to its physiological role, Gln and its transporters are also potential targets for various diseases, such as intestinal inflammation, cancer, and metabolic diseases (Avissar et al., 2004; Javed et al., 2018; Ye et al., 2018; Yadav et al., 2020). Therefore, it is important to study the exact regulatory mechanisms of intestinal Gln transport.

Although the important role of Gln in nutrition and function of the GI tract is well known (Xue et al., 2011; Li et al., 2019), the exact regulatory mechanisms of its transport in the ileum are not

fully understood. Particularly, it has not been explored if Ca$^{2+}$ signaling plays a role in this regulation. In the present study, we demonstrate for the first time that, 1) [Ca$^{2+}$]$_i$ in IEC plays an essential role in the regulation of ileal Gln-$I_{sc}$ without the involvement of the CaSR activation by Gln; 2) luminal Ca$^{2+}$ entry through apical VGCC to regulate ileal Na$^+$/Gln co-transport; 3) serosal Ca$^{2+}$ entry through TRPV1/2, SOC channels, and NCX to mediate ileal Na$^+$/Gln co-transport; 4) the ER Ca$^{2+}$ release via the RyR and IP$_3$R may also trigger ileal Na$^+$/Gln co-transport. Therefore, our findings not only reveal the important role of [Ca$^{2+}$]$_i$ in the regulation of ileal Gln transport but also provide new insights into the mechanisms of Ca$^{2+}$-mediated nutrient absorption in the ileum.

Most studies on intestinal nutrient absorption (such as dipeptide and glucose) focus on the proximal small intestine (such as the duodenum and the jejunum) but not on the distal small intestine (such as the ileum). However, the ileum is the longest segment of the intestine, where the chyme has the longest residence time to complete nutrient absorption. Our study also showed that Gln induced faster and larger $I_{sc}$ in the ileum than in the proximal intestine.

As a well-known second messenger, [Ca$^{2+}$]$_i$ regulates many physiological functions in mammalian cells, such as neural activity, hormone secretion, muscle cell contraction, etc. Yet, studies on Ca$^{2+}$ regulation of intestinal nutrient absorption are rare, particularly, the survey on Ca$^{2+}$ regulation of ileal Gln transport is still lacking. The ileum is involved in the active Ca$^{2+}$ transport when luminal Na$^+$ coupled-nutrients are high

**FIGURE 8 |** The NKA and NCX in $Ca^{2+}$-mediated Gln transport. **(A)** Representative time courses and summary data showing the effect of serosal (s) addition of ouabain [Ouabain (s), 1 mM, $n = 6$] (indicated by the red arrow) on Gln-induced $I_{sc}$, compared to a control group (Ctrl, $n \geq 6$) without any drug treatment. **(B)** Representative time courses and summary data showing the effect of serosal addition of SN-6 [SN-6 (s), 10 μM, $n = 6$] on Gln-stimulated $I_{sc}$ (indicated by the red arrow). Ctrl ($n \geq 6$) is the control group without drug treatment. Results are presented as mean ± S.E. NS, no significant differences, ****$p < 0.0001$ *vs.* corresponding control by Student's unpaired, two-tailed *t*-test.

(Kellett 2011), and it may play a more important role than the duodenum in adapting to hypocalcemia (Dhawan et al., 2017). Therefore, it is reasonable to speculate that $Ca^{2+}$ and Na⁺/Gln co-transport might interact in the ileum. In the present study, we are the first to apply the native ileum of mice to investigate the $Ca^{2+}$ regulation of ileal Gln transport and found an essential role of $Ca^{2+}$ for this regulation.

There are two primary sources of $Ca^{2+}$ in the cytoplasm in IEC: extracellular $Ca^{2+}$ entry *via* plasma membrane and intracellular $Ca^{2+}$ release from the endoplasmic reticulum (ER). The VGCC has been reported to express on the luminal side of jejunal and ileal epithelium in mice (Reyes-Fernandez and Fleet 2015; Beggs et al., 2019). We reveal that $Ca^{2+}$ entry through luminal VGCC plays a key role in Gln transport, consistent with our previous jejunal glucose absorption report. Like in the process of jejunal Na⁺/glucose co-transporter, ileal Gln transport *via* Na⁺/Gln co-transporter also depolarizes plasma membrane to induce $Ca^{2+}$ entry through luminal VGCC (Kellett 2011; Nakamura et al., 2020). The $Ca^{2+}$ entry may activate inositol 1,4,5-triphosphate receptor ($IP_3R$) and ryanodine receptor (RyR) to trigger the ER $Ca^{2+}$ release (so-called CICR) (Rahman 2012; Zhang et al., 2021). Indeed, ileal Gln-$I_{sc}$ is inhibited by either the ER $Ca^{2+}$ depletion with CPA and TPEN or inhibition of $IP_3$ production and selective blockade of RyR. ER $Ca^{2+}$ depletion

leads to extracellular $Ca^{2+}$ entry, known as the SOCE mechanism, which plays a key role in regulating $Ca^{2+}$-dependent biological functions in IEC, such as in jejunal glucose absorption (Zhang et al., 2021) and ileal Gln transport here.

Moreover, several ion channels and transporters express and function on the basolateral side of the small intestinal epithelium (Dong et al., 2005; Tsuchiya et al., 2014; Manneck et al., 2021, Yinghui Cui1 2021). Recently, the expression and function of transient receptor potential (TRP) channels in the GI tract have attracted extensive attention; TRPV1-6 channels have been shown to be stably expressed in IEC as non-selective cation channels with Na⁺ and $Ca^{2+}$ permeability (Voets et al., 2004; Rao et al., 2006; Ueda et al., 2009; Fothergill et al., 2016; Maurino et al., 2020; Manneck et al., 2021). Although TRPV channels in GI sensory neurons have been studied extensively (De Petrocellis et al., 2012; Maurino et al., 2020; Grover et al., 2021), our study is the first to demonstrate the involvement of $Ca^{2+}$ entry *via* TRPV channels in the regulation of ileal Gln transport in IEC. Na⁺/$Ca^{2+}$ influx mediated by TRPV channels could activate bidirectional ion exchange (NCX), whose transport direction depends on Na⁺ and $Ca^{2+}$ gradients and membrane potentials (Zhang J. et al., 2019; Zhao et al., 2021). Furthermore, we found that NKA on the serosal side of the intestine are also involved in ileal Gln-$I_{sc}$, although it is well
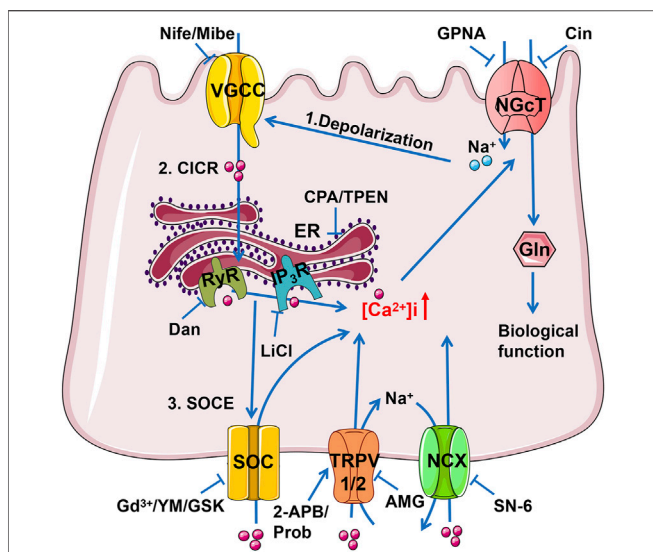
**FIGURE 9 |** The schematic diagram depicts the mutual achievement of $Ca^{2+}$ and Gln transport in the ileum. Gln entry through electrogenic $Na^+$/Gln co-transporter causes apical membrane depolarization, which activates VGCC causing $Ca^{2+}$ influx. $Ca^{2+}$ flowing from VGCC can activate $IP_3R$ and RyR mediated ER $Ca^{2+}$ release (CICR), and the depleted $Ca^{2+}$ storage may activate SOC channels to complete the SOCE mechanism of more $Ca^{2+}$ inflow. The raised $[Ca^{2+}]_i$ activates TRPV1/2 channels, leading to not only $Ca^{2+}$ entry but $Na^+$ entry as well. $Na^+$ entry would reverse NCX to further enhance $Ca^{2+}$ entry. Finally, the raised $[Ca^{2+}]_i$ promotes ileal $Na^+$ and Gln entry via NGcT. Gln, Glutamine; NGcT, $Na^+$/Gln co-transporters; ER, endoplasmic reticulum; RyR, ryanodine receptor; $IP_3R$, inositol 1,4,5-triphosphate receptor; SOC, store-operated $Ca^{2+}$ channel; TRPV, transient receptor potential vanilloid channel; NCX, $Na^+$/$Ca^{2+}$ exchanger.

known that NKA activity is essential to provide potential energy for epithelial ion transports. Therefore, we have identified two $Ca^{2+}$-permeable channels and two ion transporters on the serosal side of the ileum, which likely work together to regulate intestinal $Ca^{2+}$-dependent Gln-$I_{sc}$. $[Ca^{2+}]_i$ has a variety of possibilities in regulating Gln transport solely or synergistically: on the one hand, studies have shown that the $Ca^{2+}$-activated PKC directly regulates Gln transporters (Dong et al., 2018). On the other hand, $Ca^{2+}$ has been shown to stimulate NKA or $K^+$ channels to maintain potential differences across apical membranes for $Na^+$-coupled nutrient transport (Nepal et al., 2021).

Using native intestinal tissues we have provided functional evidence that the transport of dietary Gln and $Ca^{2+}$ is mutually regulated in the ileum. **Figure 9** depicts the proposed mechanisms of this mutual regulation: 1) the $Na^+$ entry via electrogenic $Na^+$-Gln co-transporter depolarizes the apical membrane to cause $Ca^{2+}$ entry via VGCC in IEC, triggering the CICR via $IP_3R$ and RyR; 2) the ER/$Ca^{2+}$ release induces the SOCE mechanism to activate TRPV1/2 channels, leading to not

only $Ca^{2+}$ entry but $Na^+$ entry; 3) $Na^+$ entry would reverse NCX to further enhance $Ca^{2+}$ entry; 4) the raised $[Ca^{2+}]_i$ finally promotes ileal Gln entry via $Na^+$-Gln co-transporter. There may be an alternative explanation that calcium channels are regulated by Gln via the CaSR, however, our data have clearly excluded this alternative explanation, further supporting the notion described above that is consistent with a recent report in IEC (Nakamura et al., 2020).

In conclusion, we uncovered a novel $Ca^{2+}$ regulatory mechanism of ileal Gln transport. Since Gln is intestinal fuel and has multiple biological functions in the GI tract, the $Ca^{2+}$ regulation of ileal Gln transport may be significant in GI health and disease. The combining application of $Ca^{2+}$ and Gln in enteral and parenteral solutions or targeting the corresponding channels may have therapeutic potentials to improve GI nutrition and function.

## DATA AVAILABILITY STATEMENT

The original contributions presented in the study are included in the article/**Supplementary Material**, further inquiries can be directed to the corresponding authors.

## ETHICS STATEMENT

The animal study was reviewed and approved by the Army Medical University Committee.

## AUTHOR CONTRIBUTIONS

HD conceived the study, designed and supervised the experiments, wrote, and finalized the manuscript. HW designed some experiments and finalized the manuscript. FC performed the experiments and data analysis, and wrote the draft. WX and ML supervised some experiments.

## FUNDING

## SUPPLEMENTARY MATERIAL

The Supplementary Material for this article can be found online at: https://www.frontiersin.org/articles/10.3389/fphar.2022.816133/full#supplementary-material

# REFERENCES

Allais, L., Verschuere, S., Maes, T., De Smet, R., Devriese, S., Gonzales, G. B., et al. (2020). Translational Research into the Effects of Cigarette Smoke on Inflammatory Mediators and Epithelial TRPV1 in Crohn's Disease. *PLoS One* 15 (8), e0236657. doi:10.1371/journal.pone.0236657

Avissar, N. E., Ziegler, T. R., Toia, L., Gu, L., Ray, E. C., Berlanga-Acosta, J., et al. (2004). ATB0/ASCT2 Expression in Residual Rabbit Bowel Is Decreased after Massive Enterectomy and Is Restored by Growth Hormone Treatment. *J. Nutr.* 134 (9), 2173–2177. doi:10.1093/jn/134.9.2173

Beggs, M. R., Lee, J. J., Busch, K., Raza, A., Dimke, H., Weissgerber, P., et al. (2019). TRPV6 and Cav1.3 Mediate Distal Small Intestine Calcium Absorption before Weaning. *Cell Mol Gastroenterol Hepatol* 8 (4), 625–642. doi:10.1016/j.jcmgh.2019.07.005

Bröer, A., Rahimi, F., and Bröer, S. (2016). Deletion of Amino Acid Transporter ASCT2 (SLC1A5) Reveals an Essential Role for Transporters SNAT1 (SLC38A1) and SNAT2 (SLC38A2) to Sustain Glutaminolysis in Cancer Cells. *J. Biol. Chem.* 291 (25), 13194–13205. doi:10.1074/jbc.M115.700534

Bröer, S., and Fairweather, S. J. (2019). Amino Acid Transport across the Mammalian Intestine. *Compr. Physiol.* 9 (1), 343–373. doi:10.1002/cphy.c170041

Chen, S., Xia, Y., Zhu, G., Yan, J., Tan, C., Deng, B., et al. (2018). Glutamine Supplementation Improves Intestinal Cell Proliferation and Stem Cell Differentiation in Weanling Mice. *Food Nutr. Res.* 62. doi:10.29219/fnr.v62.1439

Chen, Y., Dinges, M. M., Green, A., Cramer, S. E., Larive, C. K., and Lytle, C. (2020). Absorptive Transport of Amino Acids by the Rat colon. *Am. J. Physiol. Gastrointest. Liver Physiol.* 318 (1), G189–G202. doi:10.1152/ajpgi.00277.2019

Curi, R., Lagranha, C. J., Doi, S. Q., Sellitti, D. F., Procopio, J., Pithon-Curi, T. C., et al. (2005). Molecular Mechanisms of Glutamine Action. *J. Cel Physiol* 204 (2), 392–401. doi:10.1002/jcp.20339

Danthi, S. J., Liang, B., Smicker, O., Coupland, B., Gregory, J., Gefteas, E., et al. (2019). Identification and Characterization of Inhibitors of a Neutral Amino Acid Transporter, SLC6A19, Using Two Functional Cell-Based Assays. *SLAS Discov.* 24 (2), 111–120. doi:10.1177/2472555218794627

De Petrocellis, L., Orlando, P., Moriello, A. S., Aviello, G., Stott, C., Izzo, A. A., et al. (2012). Cannabinoid Actions at TRPV Channels: Effects on TRPV3 and TRPV4 and Their Potential Relevance to Gastrointestinal Inflammation. *Acta Physiol. (Oxf)* 204 (2), 255–266. doi:10.1111/j.1748-1716.2011.02338.x

Dhawan, P., Veldurthy, V., Yehia, G., Hsaio, C., Porta, A., Kim, K. I., et al. (2017). Transgenic Expression of the Vitamin D Receptor Restricted to the Ileum, Cecum, and Colon of Vitamin D Receptor Knockout Mice Rescues Vitamin D Receptor-dependent Rickets. *Endocrinology* 158 (11), 3792–3804. doi:10.1210/en.2017-00258

Dong, H., Sellers, Z. M., Smith, A., Chow, J. Y., and Barrett, K. E. (2005). Na(+)/Ca(2+) Exchange Regulates Ca(2+)-dependent Duodenal Mucosal Ion Transport and HCO(3)(-) Secretion in Mice. *Am. J. Physiol. Gastrointest. Liver Physiol.* 288 (3), G457–G465. doi:10.1152/ajpgi.00381.2004

Dong, W., Todd, A. C., Bröer, A., Hulme, S. R., Bröer, S. B., and Billups, B. (2018). PKC-mediated Modulation of Astrocyte SNAT3 Glutamine Transporter Function at Synapses In Situ. *Int. J. Mol. Sci.* 19 (4). doi:10.3390/ijms19040924

Ducroc, R., Sakar, Y., Fanjul, C., Barber, A., Bado, A., and Lostao, M. P. (2010). Luminal Leptin Inhibits L-Glutamine Transport in Rat Small Intestine: Involvement of ASCT2 and B0AT1. *Am. J. Physiol. Gastrointest. Liver Physiol.* 299 (1), G179–G185. doi:10.1152/ajpgi.00048.2010

Fothergill, L. J., Callaghan, B., Rivera, L. R., Lieu, T., Poole, D. P., Cho, H. J., et al. (2016). Effects of Food Components that Activate TRPA1 Receptors on Mucosal Ion Transport in the Mouse Intestine. *Nutrients* 8 (10). doi:10.3390/nu8100623

Grover, M., Berumen, A., Peters, S., Wei, T., Breen-Lyles, M., Harmsen, W. S., et al. (2021). Intestinal Chemosensitivity in Irritable Bowel Syndrome Associates with Small Intestinal TRPV Channel Expression. *Aliment. Pharmacol. Ther.* 54 (9), 1179–1192. doi:10.1111/apt.16591

He, L., Yin, Y., Li, T., Huang, R., Xie, M., Wu, Z., et al. (2013). Use of the Ussing Chamber Technique to Study Nutrient Transport by Epithelial Tissues. *Front. Biosci. (Landmark Ed.* 18, 1266–1274. doi:10.2741/4178

Hempstock, W., Ishizuka, N., and Hayashi, H. (2021). Functional Assessment of Intestinal Tight Junction Barrier and Ion Permeability in Native Tissue by Ussing Chamber Technique. *J. Vis. Exp.* 171. doi:10.3791/62468

Hu, H. Z., Gu, Q., Wang, C., Colton, C. K., Tang, J., Kinoshita-Kawada, M., et al. (2004). 2-aminoethoxydiphenyl Borate Is a Common Activator of TRPV1, TRPV2, and TRPV3. *J. Biol. Chem.* 279 (34), 35741–35748. doi:10.1074/jbc.M404164200

Javed, K., Cheng, Q., Carroll, A. J., Truong, T. T., and Bröer, S. (2018). Development of Biomarkers for Inhibition of SLC6A19 (B⁰AT1)-A Potential Target to Treat Metabolic Disorders. *Int. J. Mol. Sci.* 19 (11). doi:10.3390/ijms19113597

Joshi, S., Tough, I. R., and Cox, H. M. (2013). Endogenous PYY and GLP-1 Mediate L-Glutamine Responses in Intestinal Mucosa. *Br. J. Pharmacol.* 170 (5), 1092–1101. doi:10.1111/bph.12352

Kellett, G. L. (2011). Alternative Perspective on Intestinal Calcium Absorption: Proposed Complementary Actions of Ca(v)1.3 and TRPV6. *Nutr. Rev.* 69 (7), 347–370. doi:10.1111/j.1753-4887.2011.00395.x

Leke, R., Escobar, T. D., Rao, K. V., Silveira, T. R., Norenberg, M. D., and Schousboe, A. (2015). Expression of Glutamine Transporter Isoforms in Cerebral Cortex of Rats with Chronic Hepatic Encephalopathy. *Neurochem. Int.* 88, 32–37. doi:10.1016/j.neuint.2015.03.005

Li, M., Oshima, T., Ito, C., Yamada, M., Tomita, T., Fukui, H., et al. (2019). Glutamine Blocks Interleukin-13-Induced Intestinal Epithelial Barrier Dysfunction. *Digestion*, 1–10. doi:10.1159/000502953

Liu, G., Ren, W., Fang, J., Hu, C. A., Guan, G., Al-Dhabi, N. A., et al. (2017). L-glutamine and L-Arginine Protect against Enterotoxigenic *Escherichia coli* Infection via Intestinal Innate Immunity in Mice. *Amino Acids* 49 (12), 1945–1954. doi:10.1007/s00726-017-2410-9

Manneck, D., Braun, H. S., Schrapers, K. T., and Stumpff, F. (2021). TRPV3 and TRPV4 as Candidate Proteins for Intestinal Ammonium Absorption. *Acta Physiol. (Oxf)* 233 (1), e13694. doi:10.1111/apha.13694

Mehrke, G., Zong, X. G., Flockerzi, V., and Hofmann, F. (1994). The Ca(++)-Channel Blocker Ro 40-5967 Blocks Differently T-type and L-type Ca++ Channels. *J. Pharmacol. Exp. Ther.* 271 (3), 1483–1488.

Michiba, K., Maeda, K., Kurimori, K., Enomoto, T., Shimomura, O., Takeuchi, T., et al. (2021). Characterization of the Human Intestinal Drug Transport with Ussing Chamber System Incorporating Freshly Isolated Human Jejunum. *Drug Metab. Dispos* 49 (1), 84–93. doi:10.1124/dmd.120.000138

Moine, L., Díaz de Barboza, G., Pérez, A., Benedetto, M., and au, N. (2017). Glutamine Protects Intestinal Calcium Absorption against Oxidative Stress and Apoptosis. *Comp. Biochem. Physiol. A. Mol. Integr. Physiol.* 212, 64–71. doi:10.1016/j.cbpa.2017.07.006

Nakamura, T., Harada, K., Kamiya, T., Takizawa, M., Küppers, J., Nakajima, K., et al. (2020). Glutamine-induced Signaling Pathways via Amino Acid Receptors in Enteroendocrine L Cell Lines. *J. Mol. Endocrinol.* 64 (3), 133–143. doi:10.1530/JME-19-0260

Nepal, N., Arthur, S., Butts, M. R., Singh, S., Palaniappan, B., and Sundaram, U. (2021). Molecular Mechanism of Stimulation of Na-K-ATPase by Leukotriene D4 in Intestinal Epithelial Cells. *Int. J. Mol. Sci.* 22 (14). doi:10.3390/ijms22147569

Oguchi, T., Suzuki, N., Hashimoto, S., Chaudhry, G. A., Chaudhry, F. A., Usami, S., et al. (2012). Inner Hair Cells of Mice Express the Glutamine Transporter SAT1. *Hear. Res.* 292 (1-2), 59–63. doi:10.1016/j.heares.2012.07.005

Okuda, T., Kadotsuji, K., Takayama, C., Hanada, K., Mukaizawa, F., Ogawara, K., et al. (2006). Involvement of Intracellular Ca2+ Dynamics in Cytoprotective Action by Amino Acids and Cytotoxicity by Sodium Laurate, an Absorption Enhancer. *J. Pharm. Sci.* 95 (10), 2256–2265. doi:10.1002/jps.20712

Rahman, T. (2012). Dynamic Clustering of IP3 Receptors by IP3. *Biochem. Soc. Trans.* 40 (2), 325–330. doi:10.1042/BST20110772

Rao, J. N., Platoshyn, O., Golovina, V. A., Liu, L., Zou, T., Marasa, B. S., et al. (2006). TRPC1 Functions as a Store-Operated Ca2+ Channel in Intestinal Epithelial Cells and Regulates Early Mucosal Restitution after Wounding. *Am. J. Physiol. Gastrointest. Liver Physiol.* 290 (4), G782–G792. doi:10.1152/ajpgi.00441.2005

Rexhepaj, R., Artunc, F., Metzger, M., Skutella, T., and Lang, F. (2007). PI3-kinase-dependent Electrogenic Intestinal Transport of Glucose and Amino Acids. *Pflugers Arch.* 453 (6), 863–870. doi:10.1007/s00424-006-0154-6

Rexhepaj, R., Grahammer, F., Völkl, H., Remy, C., Wagner, C. A., Sandulache, D., et al. (2006). Reduced Intestinal and Renal Amino Acid Transport in PDK1 Hypomorphic Mice. *FASEB J.* 20 (13), 2214–2222. doi:10.1096/fj.05-5676com

Reyes-Fernandez, P. C., and Fleet, J. C. (2015). Luminal Glucose Does Not Enhance Active Intestinal Calcium Absorption in Mice: Evidence against a Role for Ca(v) 1.3 as a Mediator of Calcium Uptake during Absorption. *Nutr. Res.* 35 (11), 1009–1015. doi:10.1016/j.nutres.2015.08.004

Shi, Y., Wang, Z. E., Wu, W., Wu, D., Wang, C., and Peng, X. (2018). Glutamine Protects Intestinal Mucosa and Promotes its Transport after Burn Injury in Rats. *Int. J. Clin. Exp. Pathol.* 11 (3), 1825–1835.

Takechi, H., Mawatari, K., Harada, N., Nakaya, Y., Asakura, M., Aihara, M., et al. (2014). Glutamine Protects the Small Intestinal Mucosa in Anticancer Drug-Induced Rat Enteritis Model. *J. Med. Invest.* 61 (1-2), 59–64. doi:10.2152/jmi.61.59

Toledo Mauriño, J. J., Furuzawa-Carballeda, J., Barreto-Zuñiga, R., Martínez Benítez, B., Granados, J., et al. (2020). TRPV Subfamily (TRPV2, TRPV3, TRPV4, TRPV5, and TRPV6) Gene and Protein Expression in Patients with Ulcerative Colitis. *J. Immunol. Res.* 2020, 2906845. doi:10.1155/2020/2906845

Tsuchiya, Y., Fujita, R., Saitou, A., Wajima, N., Aizawa, F., and Iinuma, A. (2014). [6]-gingerol Induces Electrogenic Sodium Absorption in the Rat colon via the Capsaicin Receptor TRPV1. *J. Nutr. Sci. Vitaminol (Tokyo)* 60 (6), 403–407. doi:10.3177/jnsv.60.403

Ueda, T., Yamada, T., Ugawa, S., Ishida, Y., and Shimada, S. (2009). TRPV3, a Thermosensitive Channel Is Expressed in Mouse Distal colon Epithelium. *Biochem. Biophys. Res. Commun.* 383 (1), 130–134. doi:10.1016/j.bbrc.2009.03.143

Voets, T., Nilius, B., Hoefs, S., van der Kemp, A. W., Droogmans, G., Bindels, R. J., et al. (2004). TRPM6 Forms the Mg2+ Influx Channel Involved in Intestinal and Renal Mg2+ Absorption. *J. Biol. Chem.* 279 (1), 19–25. doi:10.1074/jbc.M311201200

Wang, B., Wu, G., Zhou, Z., Dai, Z., Sun, Y., Ji, Y., et al. (2015). Glutamine and Intestinal Barrier Function. *Amino Acids* 47 (10), 2143–2154. doi:10.1007/s00726-014-1773-4

Wang, B., Wu, Z., Ji, Y., Sun, K., Dai, Z., and Wu, G. (2016). L-glutamine Enhances Tight Junction Integrity by Activating CaMK Kinase 2-AMP-Activated Protein Kinase Signaling in Intestinal Porcine Epithelial Cells. *J. Nutr.* 146 (3), 501–508. doi:10.3945/jn.115.224857

Xu, J., Zeug, A., Riederer, B., Yeruva, S., Griesbeck, O., Daniel, H., et al. (2020). Calcium-sensing Receptor Regulates Intestinal Dipeptide Absorption via Ca2+ Signaling and IKCa Activation. *Physiol. Rep.* 8 (1), e14337. doi:10.14814/phy2.14337

Xue, H., Sufit, A. J., and Wischmeyer, P. E. (2011). Glutamine Therapy Improves Outcome of *In Vitro* and *In Vivo* Experimental Colitis Models. *JPEN J. Parenter. Enteral Nutr.* 35 (2), 188–197. doi:10.1177/0148607110381407

Yadav, A., Shah, N., Tiwari, P. K., Javed, K., Cheng, Q., Aidhen, I. S., et al. (2020). Novel Chemical Scaffolds to Inhibit the Neutral Amino Acid Transporter B0AT1 (SLC6A19), a Potential Target to Treat Metabolic Diseases. *Front. Pharmacol.* 11, 140. doi:10.3389/fphar.2020.00140

Yamada, D., Kawabe, K., Tosa, I., Tsukamoto, S., Nakazato, R., Kou, M., et al. (2019). Inhibition of the Glutamine Transporter SNAT1 Confers Neuroprotection in Mice by Modulating the mTOR-Autophagy System. *Commun. Biol.* 2, 346. doi:10.1038/s42003-019-0582-4

Ye, J., Huang, Q., Xu, J., Huang, J., Wang, J., Zhong, W., et al. (2018). Targeting of Glutamine Transporter ASCT2 and Glutamine Synthetase Suppresses Gastric Cancer Cell Growth. *J. Cancer Res. Clin. Oncol.* 144 (5), 821–833. doi:10.1007/s00432-018-2605-9

Yinghui, F. C., Yin3, Kai., Wan1, H., and Hui, D. (2021). Role of Serosal TRPV4-Constituted SOCE Mechanism in Secretagogues-Stimulated Intestinal Epithelial Anion Secretion. *Frontiers in Pharmaclology* 12, 684538. doi:10.3389/fphar.2021.684538

Zhang, F., Wan, H., Chu, F., Lu, C., Chen, J., and Dong, H. (2021). Small Intestinal Glucose and Sodium Absorption through Calcium-Induced Calcium Release and Store-Operated Ca2+ Entry Mechanisms. *Br. J. Pharmacol.* 178 (2), 346–362. doi:10.1111/bph.15287

Zhang, F., Wan, H., Yang, X., He, J., Lu, C., Yang, S., et al. (2019). Molecular Mechanisms of Caffeine-Mediated Intestinal Epithelial Ion Transports. *Br. J. Pharmacol.* 176 (11), 1700–1716. doi:10.1111/bph.14640

Zhang, J., Wei, Y., Bai, S., Ding, S., Gao, H., Yin, S., et al. (2019). TRPV4 Complexes with the Na+/Ca2+ Exchanger and IP3 Receptor 1 to Regulate Local Intracellular Calcium and Tracheal Tension in Mice. *Front. Physiol.* 10, 1471. doi:10.3389/fphys.2019.01471

Zhao, R., Liu, X., Qi, Z., Yao, X., and Tsang, S. Y. (2021). TRPV1 Channels Regulate the Automaticity of Embryonic Stem Cell-derived Cardiomyocytes through Stimulating the Na +/Ca 2+ Exchanger Current. *J. Cel Physiol* 236 (10), 6806–6823. doi:10.1002/jcp.30369

Zhu, X., Ma, K., Zhou, K., Voelkl, J., Alesutan, I., Leibrock, C., et al. (2020). Reversal of Phosphate-Induced ORAI1 Expression, Store-Operated Ca2+ Entry and Osteogenic Signaling by MgCl2 in Human Aortic Smooth Muscle Cells. *Biochem. Biophys. Res. Commun.* 523 (1), 18–24. doi:10.1016/j.bbrc.2019.11.005